Parametric Dependencies of JET LIDAR Profiles: Comparison of Ohmic-, L- and H-Modes

B Schunke, K Imre[1], K S Riedel[1].

JET Joint Undertaking, Abingdon, Oxfordshire, OX14 3EA, UK.
[1] New York University, 251 Mercier Street, New York, NY 10012-1185, USA.

Parametric Dependencies of JET LIDAR Profiles: Comparison of Ohmic-, L- and H-Modes

B Schunke, K Imre[1], K S Riedel[1].
JET Joint Undertaking, Abingdon, Oxfordshire, OX14 3EA, UK.
[1] New York University, 251 Mercier Street, New York, NY 10012-1185, USA.

1. INTRODUCTION

A statistical analysis has been performed upon sets of Ohmic, L-Mode and H-Mode electron temperature and density profiles obtained from the LIDAR Thomson Scattering Diagnostic [1] of the JET tokamak. The objective of the analysis was to determine whether the profiles could be represented in terms of the normalised flux parameter ψ and a set of the engineering parameters like plasma current I_p, toroidal field B_T, line averaged electron density $\bar{n}$, inductance ℓ_i, elongation , loop voltage V_{loop} , the edge safety factor q_{95} and z_{eff}. We intend to use the same models to predict the profile shapes for D-T discharges in JET and in ITER.

2. THE LOG-ADDITIVE PROFILE MODELS

Assuming that the electron temperature and density profiles in a tokamak depend only on the global parameters, we adopt generalised log-additive models to describe the profiles [2]. The technique is described in the following for the case of the electron temperature profile. We adopt the ansatz:

$$\ln[\theta(\psi,\bar{u})] = f_o(\psi) + \sum_{l=1}^{L} f_l(\psi) h_l(\bar{u})$$

with θ being the modelled temperature and $h_l(\bar{u}) = \left(\ln[I_p],\ln[B_t],\ln[\bar{n}],\ln[\kappa],....\right)$.

To estimate the unknown coefficients $f_l(\psi)$ we expand in B-splines: $f_l(\psi) = \sum_{k=1}^{K} \alpha_{lk}\beta_k(\psi)$ using cubic spline functions $\beta_k(\psi)$. The control variables $\bar{u}$ are normalised to their mean values in the data set and both the temperature shape and the magnitude are fitted at the same time. All spline coefficients are fitted simultaneously with a penalised least squares regression, choosing λ_l so that

$$\sum_{i,j}\left(\frac{\ln[T_i(\psi_j^i)] - \theta(\psi_j^i,\bar{u}_i)}{\sigma_{i,j}}\right)^2 + \sum_{1} \lambda_l \int_0^1 |f_1(\psi)|^2 d\psi \text{ is minimised.}$$

$T_i(\psi_j^i)$is the jth radial measurement of the ith measured temperature profile and $\sigma_{i,j}$ is the associated error. The second term is the smoothness penalty function, which damps down artificial oscillations in the estimated $f_1(\psi)$.

We use the Rice criterion to estimate the total error, which consists of variance plus smoothing bias plus the model bias (the error arising from the use of an incorrect model). The Rice criterion differs from a least square fit by the denominator and enables us to compare models and optimise a given model with respect to the smoothing parameter. Adding one parameter at a time during a sequential selection procedure and minimising

$$C_R = \frac{\sum_{i,j}\left(\left(\ln\left[T_i\left(\psi_j^i\right)\right] - \theta\left(\psi_j^i, \bar{u}_i\right)\right) / \sigma_i\right)^2}{\left(N - 2 \times \textit{degrees of freedom}\right)}$$

then defines a set of dominant variables.

The same fitting process is carried out for the density profiles. Since the line average density is a control variable, we normalise the density profiles to $\bar{n}$.

Advantages of log-additive models:

- Discharge specific phenomena are eliminated by fitting all profiles simultaneously.
- Physics insight into which global variables influence profiles.
- Compact representation for a class of discharges.
- The fitted profiles may easily be input into analysis codes.
- Extrapolation to new values of engineering parameters possible.
- Self consistent errors, including discharge variability, are estimated using repeated measurements.

3. JET ELECTRON DENSITY AND TEMPERATURE PROFILE PARAMETERISATION

We have compiled and, using the fitting method described above, statistically analysed a 43-profile Ohmic data set, a 51-profile L-Mode data set and a 51-profile H-Mode data set. The data were taken from experimental campaigns from 89 to 92. Table 1 shows the parameter ranges of the JET operating space covered.

Table 1	Ohmic	L - Mode	H-Mode
I_p / MA	1.0 - 5.0	1.0 - 4.9	2.1 - 3.2
B_T / T	1.1 -3.4	1.4 - 2.9	1.4 - 29
q_{95}	2.8 - 12.4	3 - 17	3 - 7
P_{RF} / MW	0	0 - 9.7	0 - 9.7
P_{NB} / MW	0	0 - 10.0	0 -12.4

Each profile is measured at 50 locations (every 5 cm) along the mid-plane of the JET vessel. The raw profile data show much radial structure and vary slowly in parameter. We remove the outermost points near the inner wall, where the dumping of the laser light causes a spurious spike on the profile. As the spatial resolution of the diagnostic is about 10 cm, the measurement errors are autocorrelated, and we are able to fit the data with smaller residual errors.

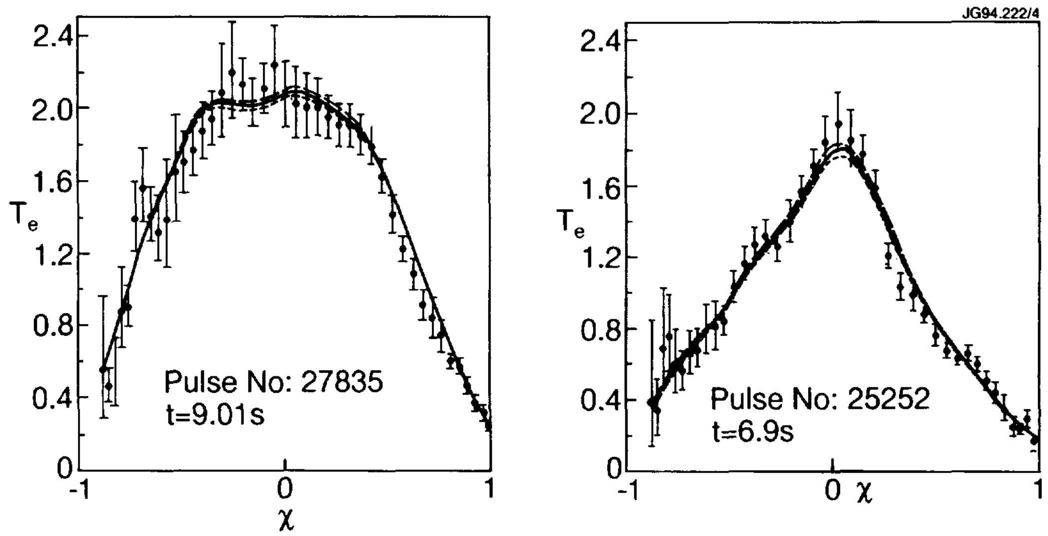

Figure 1: Examples of predicted temperature profile from model with raw data

3A. ANALYSIS OF OHMIC DISCHARGES

Table 2 visualises the selection procedure of the dominant control variables for the Ohmic data set. Fitting all candidates in a one variable fit, one finds that the current I_P minimises C_R. This parameter is then selected and paired with all other variables in a two variable fit. The variable that minimises C_R in combination with I_P is then selected as second parameter, and so on for third and fourth variable.

This sequential selection procedure shows that I_P is the most important variable in determining the plasma temperature, followed by the toroidal field B_T, the line average density $\bar{n}$ and q_{95}. Adding a fifth variable does not appreciably decrease C_R, so we choose the four variable model.

***Table 2:** Rice table for Ohmic data set - temperature profiles*

Vars in model	1 Var	2 Var	3 Var	4 Var	5 Var
$\ln[\bar{n}]$	4.64	1.73	**1.12**	seed	seed
$\ln[q_{95}]$	3.04	1.78	1.36	**0.885**	seed
$\ln[I_p]$	**1.93**	seed	seed	seed	seed
$\ln[B_T]$	3.96	**1.58**	seed	seed	seed
$\ln[\kappa]$	4.30	1.94	1.56	1.10	0.875
a	4.60	1.91	1.58	1.11	0.865
R	4.47	1.88	1.58	1.06	0.869
V_{loop}	4.63	1.92	1.53	1.10	0.875
$Z_{eff,1}$	4.01	1.91	1.55	1.06	0.872
$Z_{eff,2}$	4.37	1.79	1.57	1.11	0.85
ℓ_i	4.21	1.63	1.48	1.05	0.875
Time	4.58	1.876	1.52	0.923	0.793

The resulting model for the JET Ohmic temperature profile is:

$$\ln[T(\psi)] = f_0(\psi) + f_1(\psi)\ln[I_p/2.552] + f_B(\psi)\ln[B_T/2.710] + f_n(\psi)\ln[\bar{n}/2.1712] + f_q(\psi)\ln[q_{geo}/q]$$

with $q_{qgeo} = q_{95}I_p/B_T$ the geometric part of the safety factor q_{95}.

As seen in Figure 2 the electron temperature profile broadens and becomes slightly hollow with increasing current when the other parameters are held constant. The same effect is also seen with decreasing toroidal magnetic field for constant current. Since $f_1(\psi) \neq c - f_B(\psi)$ the profile shape does not depend exclusively on the ratio I_P/B_T. The Rice table shows that the plasma inductance is not particularly influencing the temperature.

Goodness of fit

Our best fit for Ohmic temperature profiles has an average error of 187 eV, which is 12.8 % of the typical line average temperature. The error bar for predicting new measurements is larger than the typical residual fit error. With C_R1.5 the error bar for predictions is 22% larger than the typical measurement error.

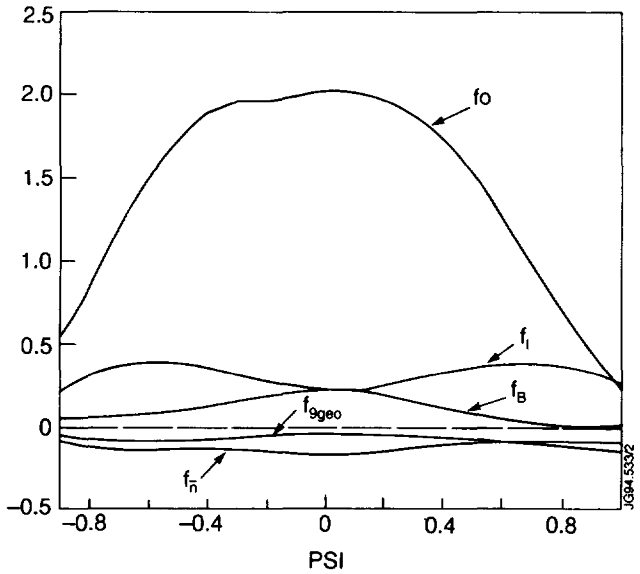

Figure 2: Spline functions for Ohmic electron temperature profiles

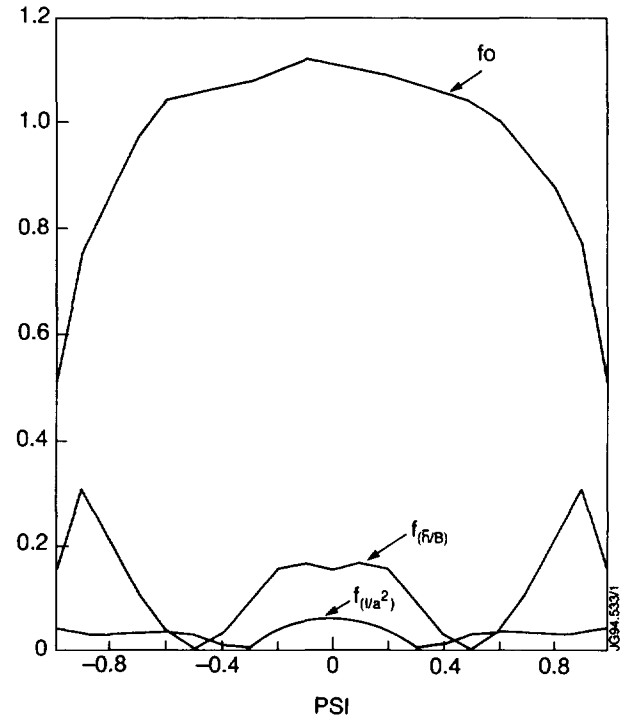

Figure 3: Spline functions for Ohmic electron density profiles

Table 3 presents the model selection criteria for Ohmic density profiles. Compared to the temperature fewer variables are necessary to model the profiles. The normalised Ohmic density profile depends significantly only on a single parameter: $\bar{n}$ / B_T, which strongly resembles the Murakami parameter, and broadens for higher $\bar{n}$ / B_T. The average current density divided by the elongation I/a^2 is the next important variable, but its influence is so minor (Figure 3), that we are inclined to drop it from the final model and instead adopt the simple expression:

$$\ln[n(\psi)/\bar{n}] = f_0(\psi) + f_{n/B}(\psi)\{\ln[\bar{n}/B_t] + 0.2215\}$$

Due to the normalisation of the density profiles, the fit error is 6.65 %, which is greatly reduced compared to the fitting of the temperature profiles. Including I/a^2 in the discription reduces the error to 6.47%.

Table 3 : Rice table for Ohmic data set - density profiles

Vars in model	1 Var	2 Var	1spline 1ct	3 Var
$\ln[\bar{n}]$	1.664	1.460	1.469	1.405
$\ln[q_{95}]$	1.799	1.424	1.472	1.396
$\ln[I_p]$	1.788	1.417	1.472	seed
$\ln[B_T]$	1.877	1.460	1.470	1.405
$\ln[\kappa]$	1.923	1.439	1.473	1.404
$B / \bar{n} R$	1.841	1.424	1.470	1.392
$q_{95}\, l_{95}/B$	1.878	1.444	1.471	1.387
V_{loop}	1.884	1.432	1.465	1.375
$Z_{eff,}$	1.816	1.362	1.469	1.332
I / a^2	1.775	**1.413**	1.472	1.394
l_i	1.774	1.445	1.472	1.407
Time	1.906	1.437	1.437	1.379
$\bar{n} / B$	**1.470**	seed	seed	seed

3B. ANALYSIS OF L- AND H-MODE DISCHARGES

We use similar log-additive model for L- and H-mode discharges, fitting unnormalised temperature and normalised density profiles. In each case, we determined the selection of control variables by minimising the Rice criterion. In particular we find

in the case of L-Mode profiles:

The dominating parameter is the heating power P_{aux}, followed by the magnetic field B_t and again the line average density.

Best fit model:

$$\ln[T(\psi)] = f_0(\psi) + f_B(\psi)\{\ln[B_t] - 0.9447\} + 0.3\{\ln[P_{aux}] - 1.3504\} - 0.4\{\ln[\bar{n}] - 0.7809\}$$

As in the case of the Ohmic discharges, the line average density is also the most important parameter for L-mode. The profiles flatten with increasing line density. We also observe a weak dependency on the elongation, (Figure 4), which is surprising as the parameter varies relatively little in the dataset. It influences mainly the edge region of the profile where the density profile decreases rapidly at higher elongations. The resulting model is:

$$\ln[n(\psi)/\bar{n}] = f_0(\psi) + f_n(\psi)\{\ln[\bar{n}] + 1.0784\} + f_\kappa(\psi)\{\ln[\kappa] - 0.51017\}$$

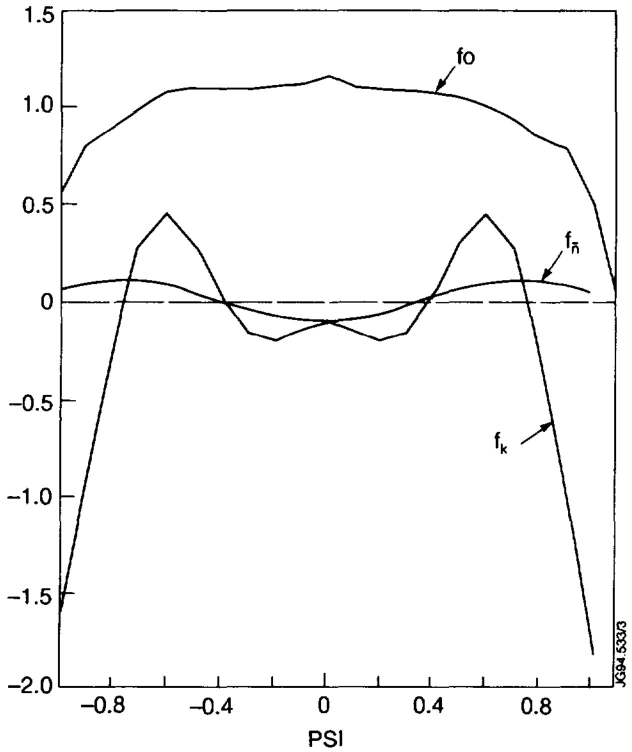

Figure 3: Spline functions for L-Mode electron density profiles

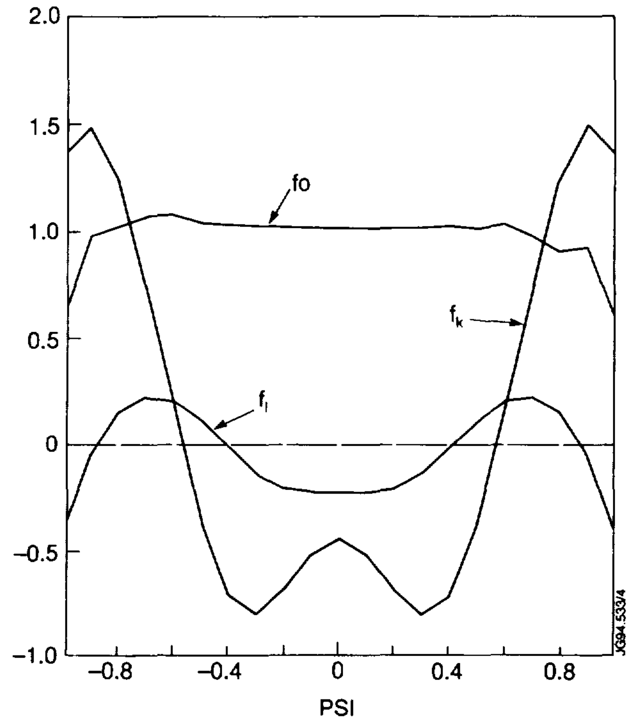

Figure 4: Spline functions for H-Mode electron density profiles

in the case of H-Mode profiles:

The H-mode temperature shape depends primarily on I_P as in the Ohmic case' followed by Z_{eff} and the additional heating power P_{aux} and q_{95}:

Best fit model:

$$\ln[T] = f_0(\psi) + 2.234\ \ln\{[I_p] - 0.9775\} + 0.1556\{Z_{eff} - 0.2633\} + 0.118\ \{\ln[P_{aux}] - 0.1960\} + f_q(\psi)\{\ln[q_{95}] - 0.1619\}$$

The current I_p is the most important control variable for the normalised H-mode density, followed by the elongation . Increasing Ip results in less peaked, sometimes hollow profiles. Increasing extends the flat regions of the profile, resulting in sharper gradients in the edge region. The range of variation of is small (14.5% for H-mode) in the dataset and the effect might be weaker in a larger sample size. Best fit model:

$$\ln[n(\psi)] = f_0(\psi) + f_1(\psi)\{\ln[I_p] + 0.9775\} + f_\kappa(\psi)\{\ln[\kappa] - \}$$

4. FUTURE WORK

Extension of JET profile data base to further clarify parametric dependencies. Especially include and compare to profiles from new divertor configuration.
Multimachine database for extrapolation to ITER performance possible.
Testing of alternative log-additive diffusivity model for plasma profiles, with the temperature profile shape resulting from a radial distribution of sinks and sources.

Hierarchy of models

Profile resilience and diffusivity profile resilience strongly suggest that the appropriate empirical models for local profile dependencies are the additive log-temperature model and the additive log-diffusivity model. We therefore distinguish four classes of empirical transport models:

1) Global confinement models: τ_E = f (engineering variables)
2) Semiparametric profile models: T = f (ψ,engineering variables)
3) Semiparametric diffusivity models: χ = f (ψ,engineering variables)
4) First principal transport models: T = f (physics variables), possibly given by theoretical expressions.

5. REFERENCES:

[1] H.Salzmann, J.Bundgaard, A.Gadd, et.al., Rev.Sci.Instrum.**59**, 1451(1988)
[2] McCarthy, P.J., Riedel, K.S., Kardaun, O.J.W.F., Murmann, H., Lackner, K., Nuclear Fusion, **31**, 1595 (1991)